atmosphere

Article

Interference of Urban Morphological Parameters in the Spatiotemporal Distribution of PM_{10} and NO_2, Taking Dalian as an Example

Yuan Su [1,*], Xuezheng Wu [1], Qinfeng Zhao [2], Dian Zhou [3] and Xiangzhao Meng [3]

[1] School of Architecture & Fine Art, Dalian University of Technology, Dalian 116024, China; wxz@mail.dlut.edu.cn
[2] Faculty of Environmental Engineering, The University of Kitakyushu, Kitakyushu 8080135, Japan; b0dbb414@eng.kitakyu-u.ac.jp
[3] School of Human Settlements and Civil Engineering, Xi'an Jiaotong University, Xi'an 710054, China; dian-z@mail.xjtu.edu.cn (D.Z.); xzmeng@xjtu.edu.cn (X.M.)
* Correspondence: suyuan@dlut.edu.cn; Tel.: +86-1566-8685-619

Abstract: Recently, air quality has become a hot topic due to its profound impact on the quality of the human living environment. This paper selects the tourist city of Dalian as the research object. The concentration and spatial distribution of PM_{10} and NO_2 in the main urban area were analyzed during the peak tourist seasons in summer and winter. Simulations were used to explore the spatial and temporal variation patterns of PM_{10} and NO_2, combining building and road density at different scales to reveal the coupling relationship between individual pollutant components and urban parameters. The results show that the PM_{10} concentration is high in the center and NO_2 is concentrated in the northern district of Dalian City. In an area with a radius of 100 m, the dilution ratio of building density and road density to the concentration of the PM_{10} pollutants is at least 43%. Still, the concentration of NO_2 is only coupled with road density. This study reveals the spatial and temporal variation patterns of PM_{10} and NO_2 in Dalian, and finds the coupling relationship between the two pollutants and building density and road density. This study provides a reference for preventing and controlling air pollution in urban planning.

Keywords: spatiotemporal distribution; pollutant concentration; road density; building density

check for updates

Citation: Su, Y.; Wu, X.; Zhao, Q.; Zhou, D.; Meng, X. Interference of Urban Morphological Parameters in the Spatiotemporal Distribution of PM_{10} and NO_2, Taking Dalian as an Example. *Atmosphere* **2022**, *13*, 907. https://doi.org/10.3390/atmos13060907

Academic Editors: Zhenbo Wang and Kexin Li

Received: 12 May 2022
Accepted: 30 May 2022
Published: 2 June 2022

1. Introduction

The rapid development of urbanization has generated economic prosperity and various air pollution problems. From 2016 to 2018, China's air environmental quality ranked second to last in the Global Environmental Performance Index (EPI) report [1]. Urban air quality as an evaluation indicator has a profound impact on the comfort, physical and mental health of people in their living environment. Air pollution is composed of numerous particulate pollutants. The variation of the emission source and strengths can also affect the distribution of the air pollutants. The distribution of contaminants in China shows that a high pollutant concentration is caused by the discharge of developed industrial areas, not the population density [2]. Residents who migrate from rural to urban areas in China often take generations to settle down in highly urbanized, modern cities [3]. In addition, the urbanization process is accompanied by the construction of many roads and buildings. Urban morphological parameters are urban design elements that include many indicators such as road density, building density, and greening rate. They are constantly changing in the process of urbanization and have an essential impact on the distribution of functions of the city and residents' production and life in various regions. Improving the urban air quality through urban planning is necessary to prevent the concentration of various particulate air pollutants from exceeding the standard for a long time. Hence, it is vital to analyze the variation of individual components of contaminants and their distribution, from urban pollutant composition to urban parameters.

At present, research on urban pollutants mainly focuses on contaminants' concentration changes and spatial distribution. The air pollutants in Hangzhou, China were significantly reduced on weekends [4]. In terms of the air pollution characteristics, high concentrations of PM_{10} and ozone coexist in the same region of the Sichuan Basin and surrounding cities [5]. As an indicator for evaluating air quality, the air quality index (AQI) includes six pollutant components: PM_{10}, SO_2, O_3, $PM_{2.5}$, NO_2, and CO. Comparing the topography of cities and regions, the AQI value in North China has always been at a high level, which indicates that changes in urban topography and meteorological conditions influence pollutant concentrations [6]. China's national policy has made Dalian a key coastal tourism megacity in Northeast China. Affected by the terrain, Dalian has a well-developed transportation network, and the preservation of buildings in different periods makes Dalian rich in architectural samples [7]. The air quality can be affected by changes in the concentration of individual pollutant components. Independent analysis of each emission pollutant can accurately reflect the spatiotemporal distribution of urban pollutants, and optimize or control the urban air quality from the source.

The urban tourism policies make the air quality requirements extremely high, and reducing air pollution is remarkably beneficial to economic development. However, the proportions of PM_{10} and NO_2 in the AQI of Dalian are significantly higher than in other cities [8]. The two pollutants threaten human respiratory health and interfere with atmospheric visibility in coastal cities, and have a bidirectional causal relationship with the number of tourists [9]. This study focused on the concentrations of PM_{10} and NO_2 in Dalian due to the two pollutants failing to meet the annual average standards of the "Global Air Quality Guidelines" (AQG2021) issued by the World Health Organization (WHO) [10] and far exceeding China's ambient air quality standards (GB3095-2012) [11]. The PM_{10} and NO_2 distribution can accurately reflect the spatiotemporal distribution of urban pollutants and be used to optimize urban air quality.

Many scholars pay attention to the regional variation and method detection of PM_{10} and NO_2 pollutants. PM_{10} has a strong interaction between cities in the plain area [12]. Among them, the NO_2 in the plains of China is mainly caused by activities such as human industrial development pollution, and the PM_{10} in the west of Shanghai is mostly caused by vehicle exhaust emissions [13]. From west to east, NO_2 and PM_{10} in Hebei Province showed a gradual decline in concentration [14]. The variation range of NO_2 in the winter of Shijiazhuang is higher than in other seasons [15], consistent with the results obtained by analyzing NO_2 concentration data [16].

Regarding detecting pollutant concentration, the NO_2 variation model predicted by the data-network method confirmed that the areas with high pollutant concentrations were concentrated in large urban agglomerations from 2014 to 2019 [17]. This result is consistent with the conclusion drawn by deep learning to establish the calculation model of mass air distribution [18]. Sofia also verified and analyzed the air quality and bioclimatic indices through computer simulation [19].

The pollutant components have essential impacts on residents' health. The outdoor space morphological data parameters will affect the AQI [20]. The coupling relationship between temperature, humidity, wind speed, and PM_{10} concentration is substantial [21]. The geographic environment of the urban area of Beijing is correlated with carbon dioxide, and the wind speed is negatively correlated with tree height [22]. High wind speeds generate new levels of fugitive dust pollution [23], combined with pollutants in the airstream, which may lead to a significant increase in the number of COVD-19 cases [24]. In addition, changes in the location of urban blocks can lead to changes in pollutant concentrations [25]. Outdoor morphology indicators such as proximity, circularity, and vegetation coverage are closely related to pollutants [26], and the diverse land attributes affect urban air quality directly in Lanzhou [27]. In the urban center, areas with higher PM_{10} and NO_2 concentrations had higher site coverage, building height and enclosure. Compared with the sparse road network, the compact road network has a higher concentration of PM_{10} particles [28]. Cities with a single center and sparse buildings have a low particle concentration [29], and the air quality in a low-population density city is better [30]. These studies are significant for coupling urban morphological parameters and pollutants in Dalian.

In this paper, the concentrations of NO_2 and PM_{10} in Dalian were studied, and the two pollutants' temporal and spatial distribution rules were explored. Building and road density was coupled with two pollutants in areas with various radii. The results were substituted into the block scale for verification and analysis, and the linear relationship of PM_{10} concentration was compared according to additional land attributes. This paper aims to study the impact of urban spatial parameters in Dalian on air pollutants in urbanization and discuss the relationship between PM_{10} and NO_2 pollutants and road density and building density.

2. Objects and Methodology

2.1. City Data and Measured Point Settings

Dalian is located in the south of the Liaodong Peninsula of China. The Ministry of Environmental Protection assessed Dalian in 2015 and found that the air quality and ecological environment were deteriorating gradually. Dalian is often accompanied by sea fog in the temperature inversion layer and a complex topographic landscape, making the city's air pollution and source emission intensity and dispersion efficiency high. Haze and extreme weather occur frequently and do not meet the requirements. The city's tourism policy provides an extremely high demand for air quality.

Figure 1 presents the measuring points' layout in Dalian City. The diffusivity and flotation capacity of PM_{10} are weaker than NO_2 because the particle radius is more significant than that of $NO_{2.}$ The mobile recording method was used to measure PM_{10}. To compare and analyze the pollutants with different attributes in the city, the main urban area of Dalian was divided into six plots with their features, including residential land, green parkland, industrial land, commercial land, education land, and public land. The number of points of PM_{10} was set based on the area ratio of six land characteristics. Since NO_2 changes rapidly and is significantly affected by local pollution sources, fixed weather stations gathered the NO_2 data.

To avoid differences in the distribution of pollutants caused by land-use attributes, the residential land, representing the most significant proportion of the main urban area, was selected for the actual measurement. According to the distribution of residential areas in the main urban area of Dalian, 17 measuring points were set up in the 17 residential areas with the highest population density. During each quarter's actual measurement of the points, instrument damage and human sabotage occurred. Data anomalies finally occurred, and individual points were abandoned every three seasons. The distribution map of PM_{10} measured points in the summer of 2016 is shown in Figure 1. PM_{10} measuring points were distributed in 30 regions. Seventeen measuring points were set for NO_2 in the spring of 2017 and 2018.

2.2. Research Simulation Methods and Data Collection

Figure 2 presents the research flow chart of this paper. Firstly, according to the topography and urban function division of the main urban area of Dalian, the measuring points of PM_{10} were allocated to land with six attributes, while we arranged the NO_2 measuring points on the residential land, which represents largest area in the main urban area of Dalian. After collecting PM_{10} and NO_2 measurement data, we compared these data with the national control station data to verify accuracy. According to the comparison of the data, we analyzed the differences, and normalized the data. We substituted the data into ArcGIS to perform the inverse distance weighting method to obtain the spatiotemporal distribution. Where the density of road networks and buildings was higher, the concentration of pollutants was higher. Furthermore, the road density and building density at three scales around the measuring point was counted, and the data of the two pollutants were combined for analysis. Finally, the interference degree of road network density and building density on the pollutant concentration of land with different attributes was revealed.

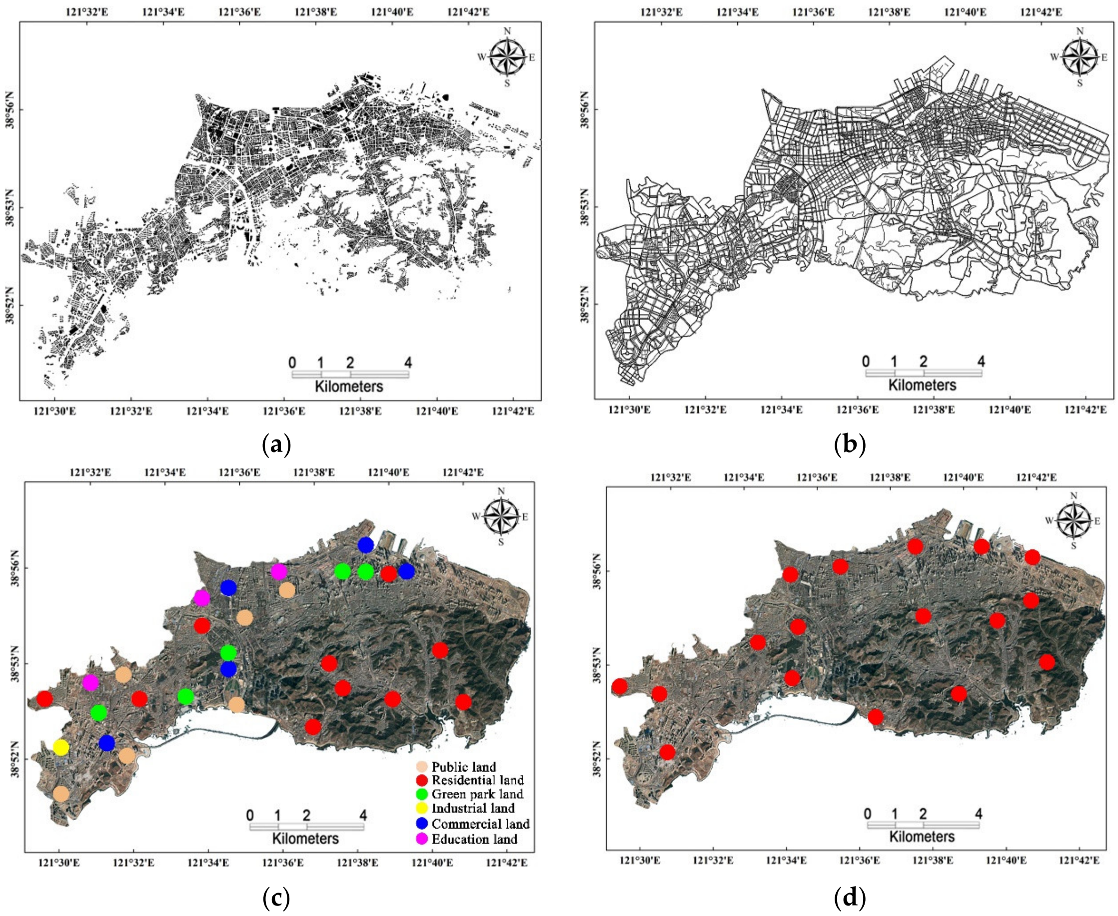

Figure 1. Measuring points' layout in Dalian City (data source: https://www.google.com/maps, accessed on 1 August 2020). (**a**) Architectural infographics of Dalian, (**b**) Road information map of Dalian, (**c**) Measured points distribution of PM_{10}, (**d**) Measured point distribution of NO_2.

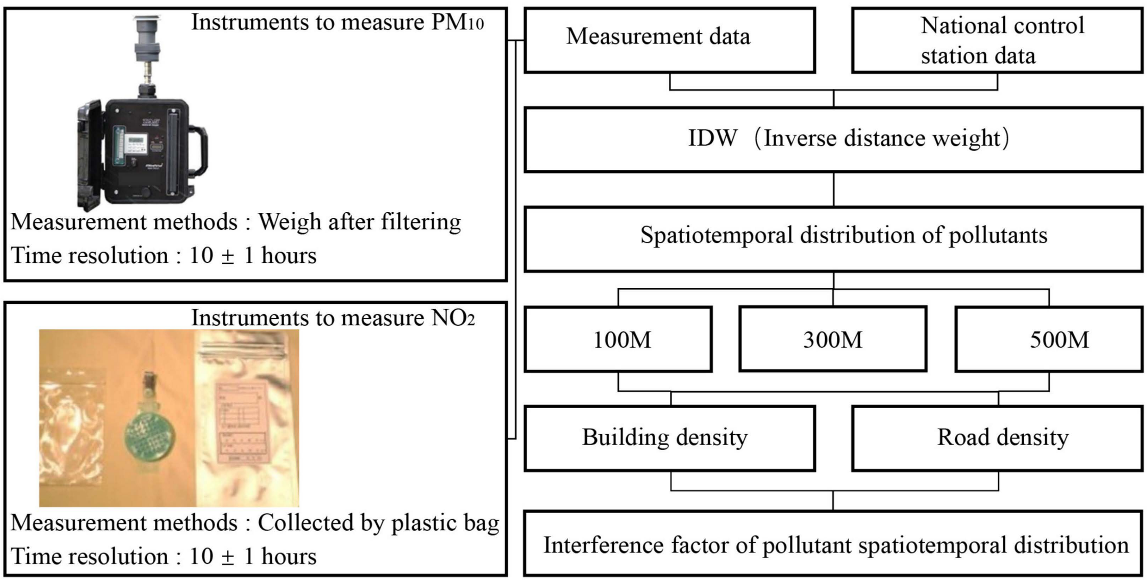

Figure 2. Research process and equipment diagram.

To monitor the concentrations of PM_{10} and NO_2 at the block scale in the living environment of urban residents, the monitoring data of PM_{10} and NO_2 concentrations were obtained by mobile and fixed sampling. As shown in Figure 2, the measurement of PM_{10} used the filter weight method, and the sampling instrument was the AIRMETRICS portable air sampler MiniVolTM from the USA. The PM_{10} sampler measures mass through an air filter to extract a quantitative volume at a pedestrian height of 1.5 m. It is captured on the filter and weighed to remove the assembly of the air filter. The NO_2 in the air was collected by the HandySONOX passive sampler and analyzed by the 42i nitrogen oxide analyzer. The sampling time was selected from 8:00 am to 6:00 pm. The time resolution was 1 h.

In cities, the primary sources of NO_2 and PM_{10} are exhaust emissions and vehicle dust, or the emissions of burning fuel from human settlement activities [31]. The concentration of NO_2 and PM_{10} changes according to the distribution of the urban road networks and the density of human settlements. From the perspective of urban planning, this paper quantified the urban road network by road density and urban population density by building density. The relationship between the two pollutant components and traffic flow and life at different scales was analyzed through the quantitative statistics of two urban morphological parameters—density correlation, revealing the specific impact value of vehicle exhaust and living density on pollutant concentration.

3. Spatial and Temporal Distribution of PM_{10} and NO_2

3.1. Analysis of PM_{10} and NO_2 Concentration Data

The pollutant concentrations at each site in order from highest to lowest are summer 2017, summer 2016, and winter 2016. The PM_{10} concentrations in the summer of 2017 and 2016 far exceeded the "China Air Environmental Quality Standard". The highest and lowest PM_{10} concentrations in winter were half of those in summer. The increase in PM_{10} concentration in the summer of 2017 was more significant than that in 2016, and the peak and trough value was three times that of the winter of 2016. Figure 3a–c show the PM_{10} concentration distribution in the measured data. The summer of 2017 was the season with the highest concentration. The highest PM_{10} measurement concentration was 339 $\mu g/m^3$ for 17S-12, and the lowest was 69 $\mu g/m^3$ for 16S-24.

Comparing the land properties, the industrial land measurement points have reduced pollution emissions due to the shutdown of industries in winter. Emissions from other categories of pollutants were lower when the cold outdoor environment interfered with people's activities. The significant difference between winter and summer air pollution in the green garden is the airflow formed by the vegetation growth cycle, which weakens the dilution effect of pollutants. The abnormality of 308 $\mu g/m^3$ in the summer of 2016 shows the weak airflow in the enclosed form of residential buildings. When the site is located below the airflow opening, the poor circulation will cause a severe accumulation of pollutants. Various location attributes strongly interfere with pollutant concentration, and the PM_{10} variation law of additional land is worthy of in-depth study.

Figure 3e is a comparison chart of NO_2 concentration in the four seasons of 2017 and 2018. The NO_2 concentrations from high to low in winter, autumn, spring, and summer. The NO_2 concentration changes in a U-shape. Figure 3f shows the comparison of the measured concentrations of NO_2. The pollution concentration data in the spring of 2017 were similar to those of the national control station. However, the data gap for 2018 remains wide. The measured sites in spring 2018 were located in areas with a high density of buildings and roads, suggesting that these two parameters profoundly affect pollutant concentrations. In addition, burning fuel for heating in winter can lead to more associated nitrogen dioxide emissions. The outdoor thermal environment is relatively poor in summer, and NO_2 emissions are lower. NO_2 emissions are greatly affected by seasons. As shown in Figure 3d,f, the PM_{10} data between the national control station and the actual measurement were different in the summer of 2017. The inconsistency suggests that normalization of the data is necessary.

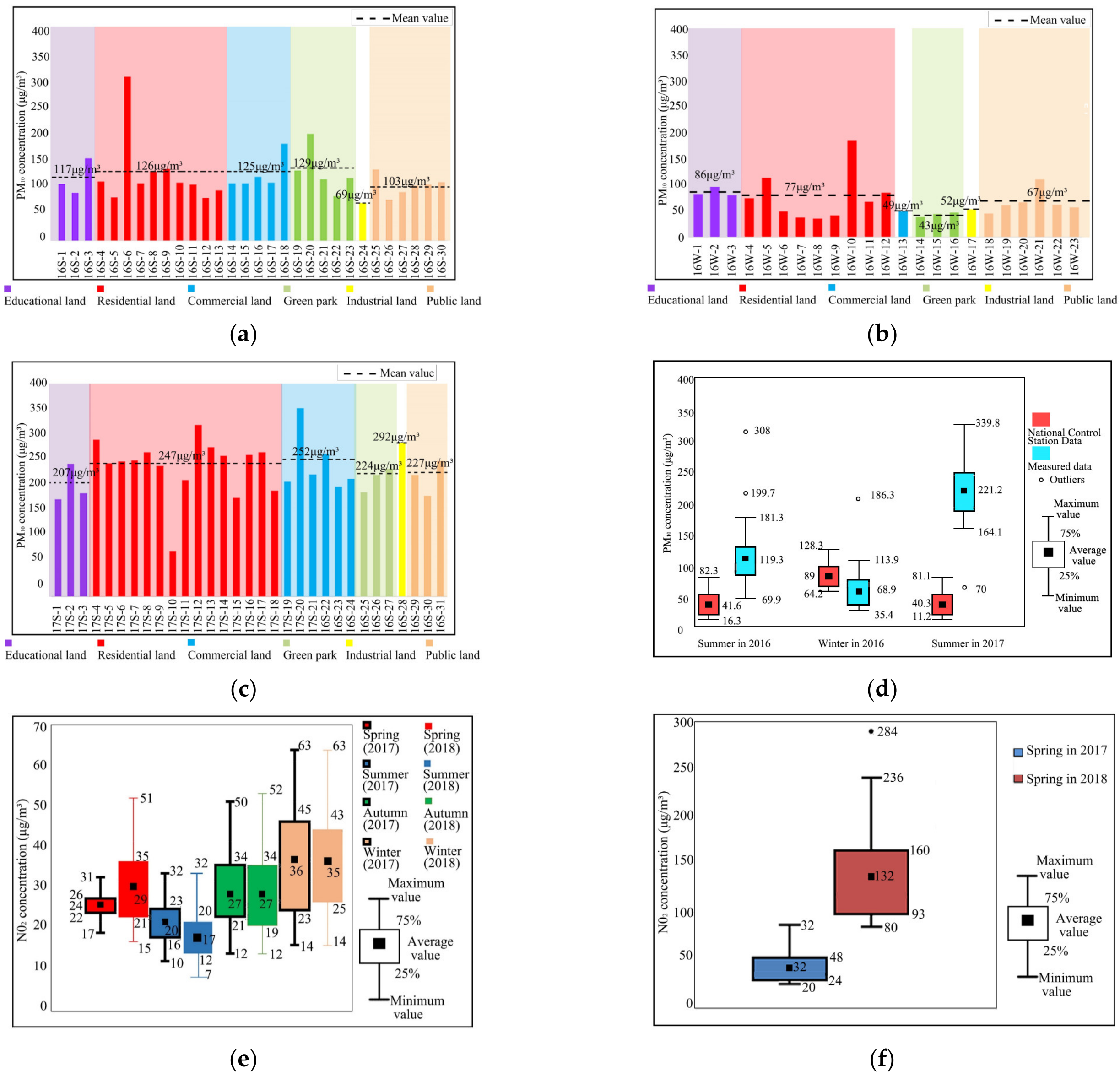

Figure 3. Comparison of measured data of NO_2 and PM_{10} with the National Control Station data. (Data source: https://www.zq12369.com/, accessed on 1 August 2020). (**a**) Measured PM_{10} in the summer of 2016, (**b**) Measured PM_{10} in the winter of 2016, (**c**) Measured PM_{10} in the summer of 2017, (**d**) Concentration comparison in three seasons, (**e**) NO_2 concentration from the National Control Station, (**f**) NO_2 concentration from measured.

3.2. Normalized Data

Given the limited number of experimental instruments and the number of participants, the data of multiple points are not completed in the same period and cannot be directly analyzed. It is necessary to revise the measurement times to the same sampling period. Using the normalized processing method normalizes the actual sampling point data. For analysis, June, July and August represent summer, and December, January and February represent winter.

3.3. PM_{10} Spatial Distribution Map

As shown in Figure 4, the measured data were used to simulate the spatiotemporal distribution of PM_{10} in the central area of Dalian through the inverse distance weighting method. Figure 4 shows the spatiotemporal distribution of PM_{10} in Dalian. The high-concentration area is located south of the main urban area. The air pollution concentration in the summer of 2017 was higher than in 2016. In the summer of 2016, the high-value areas of PM_{10} concentration in Dalian were concentrated in the central region. There are two areas with high concentration values in summer, and the overall concentration of PM_{10} in winter is low. The high concentration areas in the summer of 2016 and 2017 coincided. The highest part of the concentration in 2017 reached 356 $\mu g/m^3$, which was five times the highest value in the winter of 2016. Taking the three seasons in Figure 4 as an example, in 2016, the PM_{10} concentration in summer increased by 40% compared with winter, and the PM_{10} concentration in summer in 2017 increased by nearly 150% compared with the summer in 2016.

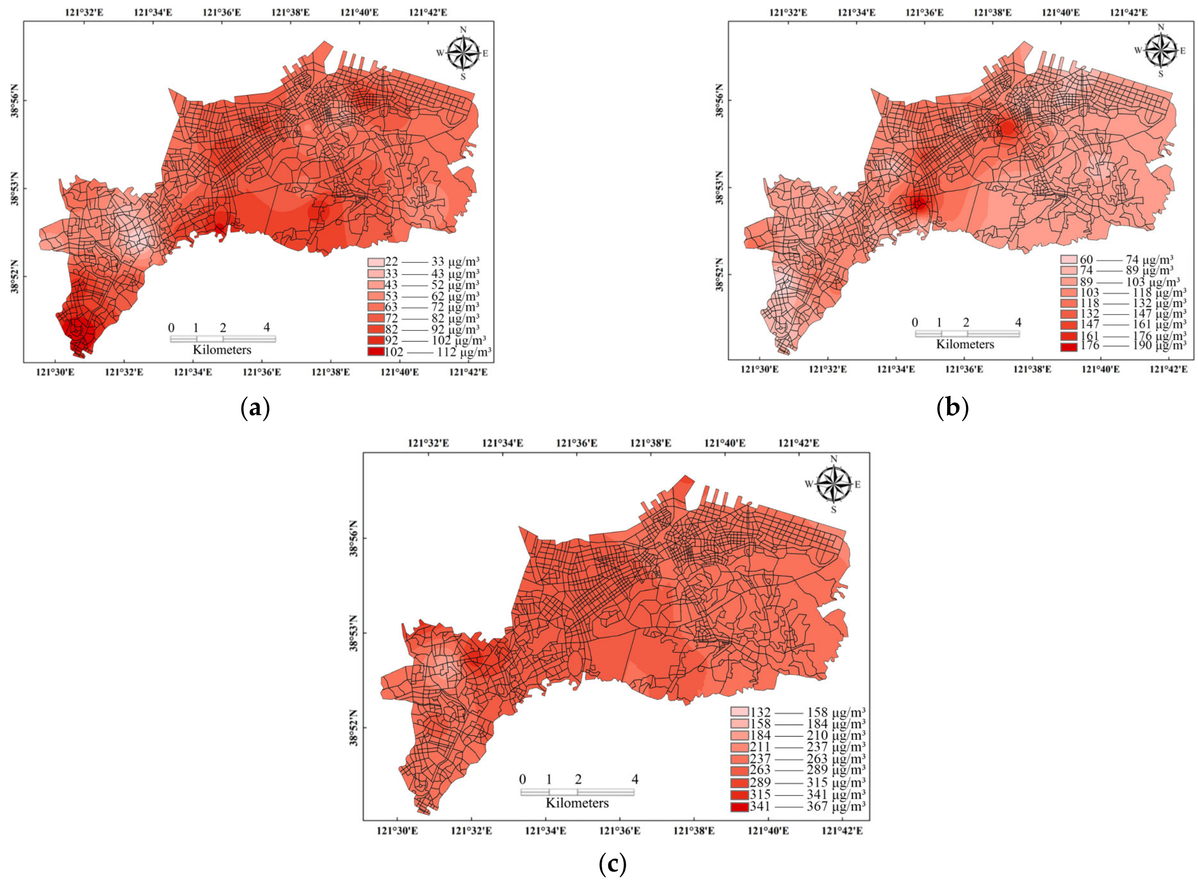

Figure 4. The distribution map of PM_{10} concentration in Dalian. (**a**) PM_{10} concentration in winter of 2016, (**b**) PM_{10} concentration in the summer of 2016, (**c**) PM_{10} concentration in the summer of 2017.

The analysis results show that the large hilly areas on the west and north sides of the main urban area of Dalian affect the flow of wind, making the conditions for pollutant diffusion in the southwestern metropolitan area poor. In addition to the impact of terrain, the exhaust emissions from vehicles in Dalian also increase the concentration of pollutants. The inconvenience of travel in winter reduces the flow of people, and the PM_{10} concentration is lower than that in summer. Under the interference of urban climate, the diffusion direction of PM_{10} changes with the urban wind direction.

3.4. NO_2 Spatial Distribution Map

Figure 5 shows the spatiotemporal distribution of NO_2 in the Dalian area. The NO_2 concentration in 2018 was higher than in 2017. The areas with high NO_2 concentrations are concentrated in the northern part of the city. Diffusion conditions of NO_2 are poor on the northeast coastline, and the highest concentration of NO_2 is 280 $\mu g/m^3$. Analysis shows that the north side is a transportation hub with high road density. The wind direction affects the diffusion direction of NO_2, with atmospheric turbulence taking away pollutants in the air. In the areas with the highest concentrations in the city, NO_2 concentrations in 2018 were more than three times higher than in 2017.

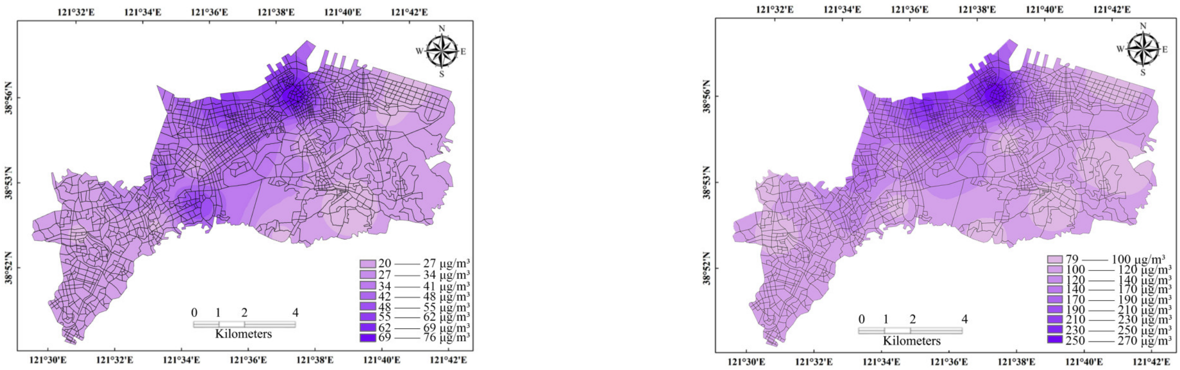

(**a**) (**b**)

Figure 5. The distribution map of NO_2 concentration in Dalian. (**a**) NO_2 concentration in the spring of 2017, (**b**) NO_2 concentration in the spring of 2018.

The analysis showed that temperature stratification and high building density resulted in slower diffusion of pollutants on the city's north side, creating high concentrations of contaminants. At the same time, the combination of high density and enclosed building complexes brings about a local urban heat island effect, which leads to higher heat capacity and minor heat consumption in the air. Therefore, the high-temperature air weakens the diffusivity of the pollutant concentration. Considering the low temperature of the sea breeze, the concentration of pollutants on the southeast coast is lower than that in the central area. Combined with the topography, the situations are diverse, such as airflow climbing, airflow sliding, and airflow backflow in the measurement area, which seriously interferes with the diffusion of pollutants. The spatial-temporal distribution results show that the city's economic center, with high population density and compact buildings, has become a high-value area of urban pollutants.

4. Linear Correlation Analysis of Pollutant Distribution

In the spatial-temporal distribution of the two pollutants in Dalian, PM_{10} and NO_2 are concentrated in the city's central area, which is economically developed with a high population density. The topography, air temperature, pressure, and pollution emissions will also affect urban pollutants. Whether the population density or the increase of pollution sources brought by urban industrialization, both are caused by urbanization. Accompanied by urbanization, building density and road density increase, the regional population congregates in the city center, and the air pollution emission increases. Economic development and industrial belts also followed, bringing vast sources of pollution. In addition, the intensification of the urban heat island effect has also increased the carrying capacity of pollutants in the air. Therefore, exploring air pollutants in Dalian is to find the relationship between urbanization and pollutants. This paper establishes the linear correlation between contaminants and the two parameters from road density and building density indicators.

4.1. Linear Correlation of Pollutant Concentration and Road Density

Figure 6 is a linear correlation diagram of pollutant concentration and road density in radius areas. According to the determination coefficient, the interference degree of road density on pollutant concentration is 100 m, 300 m and 500 m. Under the condition of 100 m, the determination coefficient of PM_{10} in the summer of 2016 was the highest, which was 0.48. In the summer of 2017, the determination coefficient of 500 m was the lowest at 0.01.

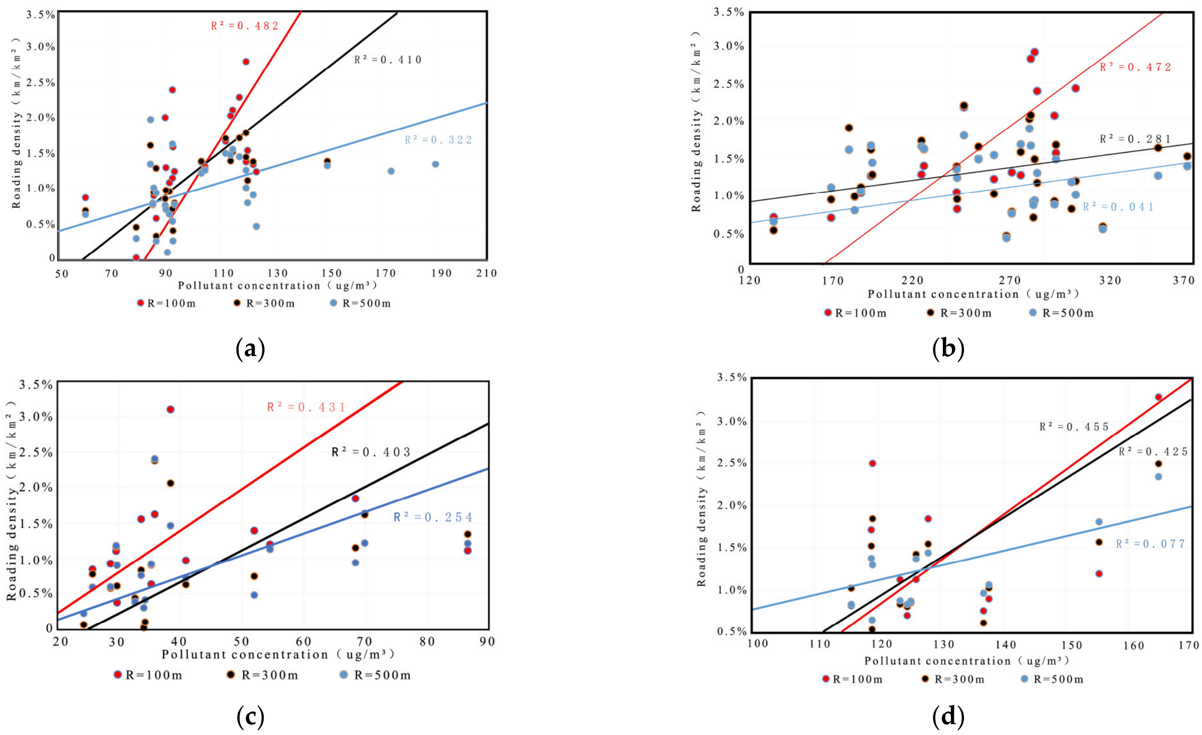

Figure 6. Linear correlation between pollutants and road density at three scales. (**a**) PM_{10} in the summer of 2016, (**b**) PM_{10} in the summer of 2017, (**c**) NO_2 in the spring of 2017, (**d**) NO_2 in the spring of 2018.

Traffic exhaust pollutants are high in areas with high road density because of residents' increased production and living density. In addition, there are many green belts in Dalian city center with high road density, a wind field inside the site surrounded by vegetation on the street, and a clockwise wind eddy in the positive pressure area on the windward side. With the disturbance of wind flow and vortex motion, the diffusion and dilution conditions of pollutants within the street becomes weaker, so the density of the road increases and pollutants spread further. The canyon effect makes dilution conditions of air pollutant concentrations harsh.

4.2. Linear Correlation of Pollutant Concentration and Building Density

Figure 7 shows the linear relationship between pollutant concentration and building density. There is a coupling relationship between PM_{10} and building density, while the coupling relationship between NO_2 and building density is very low. In the summer of 2016, the determination coefficient of building density on PM_{10} concentrations peaked within 100 m. The 300 m and 500 m scales show an attenuation trend. The highest R^2 was 0.47, and the lowest was 0.02.

The change in the wind-heat environment is caused by the building density and the wind energy blocking of the envelope structure under the condition of different radii, and is also caused by the change in the pollutant diffusion conditions. The thicker the wall, the lower the wind speed on the leeward side. The pollutants in the leeward side area are not quickly diffused, resulting in a highly polluted area in a turbulent flow. Due to the thermal effect of the air in the block, the carrying capacity of pollutants in the air in summer is higher than that in winter, and the content of air pollutants in the block in summer is increased. The linear correlation is stronger under the same diffusion conditions in a small radius area.

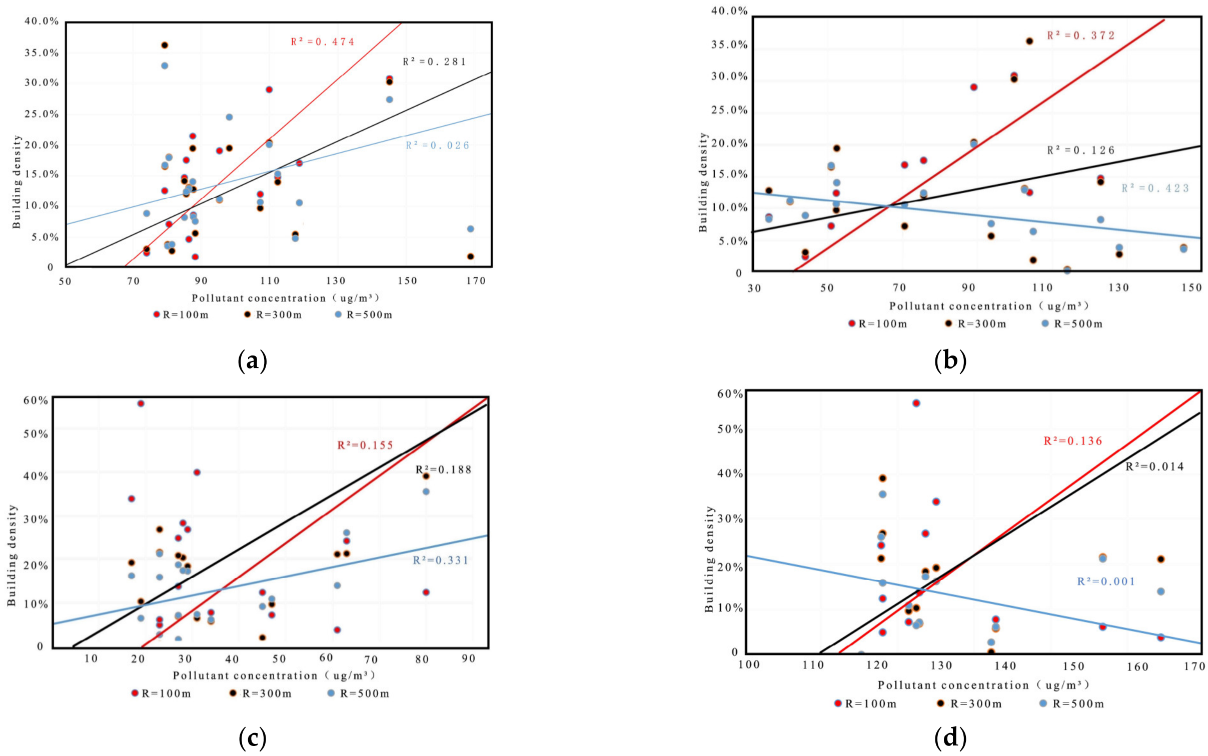

Figure 7. Linear correlation between pollutants and building density at three scales. (**a**) PM_{10} in the summer of 2016, (**b**) PM_{10} in the summer of 2017, (**c**) NO_2 in the spring of 2017, (**d**) NO_2 in the spring of 2018.

From Figure 7a,b, the linear correlation of PM_{10} concentration in winter at a radius of 500m is more significant than that at 100 m. The linear correlation between building density and PM_{10} concentration is the lowest within 300 m. Figure 7c,d shows a low linear correlation between NO_2 and building density, proving that NO_2 production is not closely related to building density. The measurement coefficient of PM_{10} under the condition of a radius of 500 m reaches 0.42, which is more than three times that under the condition of radius 100 m.

With the building density being low, the wind flowing in all directions of the city block has a good diffusion effect. When the building density increases, the unique wind corridor formed by the building will enhance the circulation capacity of the wind near the ground and improve the dilution capacity of pollutants. This result proves that regional PM_{10} concentration can be adjusted by controlling building density, referencing regional air quality.

4.3. Coupling Verification of the Pollutant Concentration at the Block Scale by Land Properties

As shown in Figure 8a, the measurement points were classified to compare the linear correlation of road density and building density with pollutant concentrations for the land properties. Statistical analysis was carried out on the measurement points with a radius of 500 m in the plot. The paper discards points with abnormal data, such as Xinghai Square, which has a very low building density. As a famous tourist attraction, the traffic flow is great and the pollutant concentration is high. The measured PM_{10} concentration verified this study in the summer of 2016. The point concentration exceeding 150 μg/m^3 was eliminated to increase the accuracy of the data.

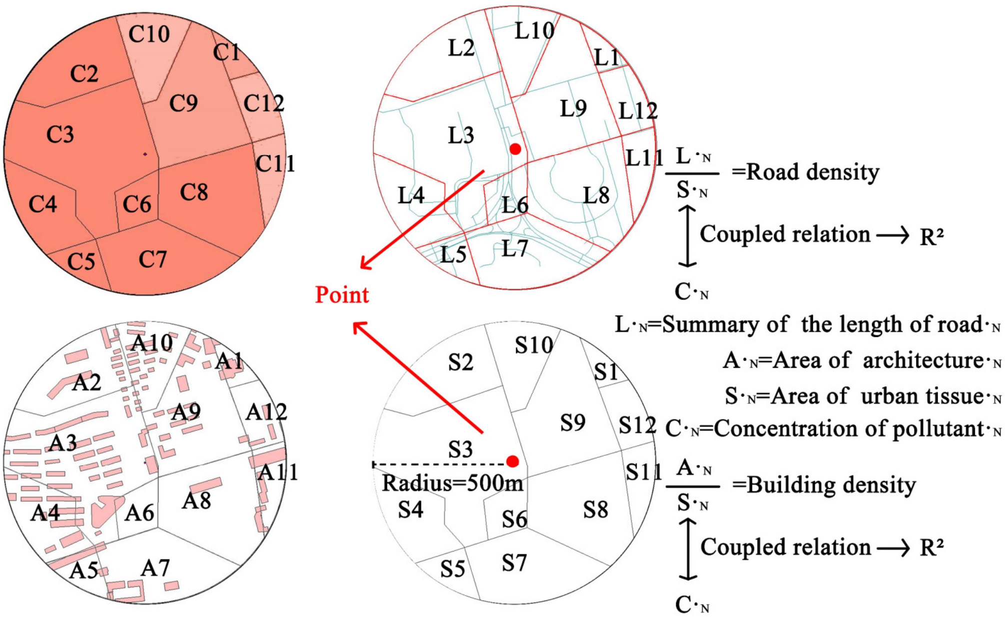

(**a**)

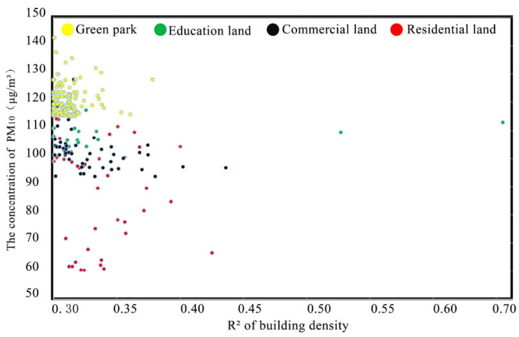

(**b**)

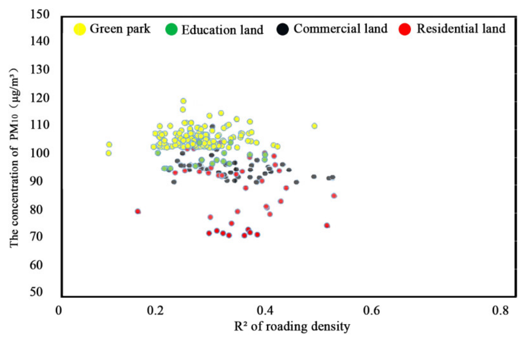

(**c**)

Figure 8. Linear correlation of PM_{10} concentration with road density and building density. (**a**) Method of verification, (**b**) PM_{10} with building density, (**c**) PM_{10} with road density.

Figure 8b,c show the determination coefficients of different attribute points and urban form parameters. According to the strength of the building density determination coefficient, these are residential, commercial, educational and urban parks. The road density determination coefficient value from low to high is in urban parks, education, commercial and residential land. The land with six attributes is divided into blocks according to the urban texture. The linear correlation between building density and PM_{10} concentration in the urban street at the measured point is the lowest among the land attributes. As shown in Figure 8c, with regard to the linear correlation of PM_{10} concentration, road density is more vital than building density. The building density in urban parks is low, and the pollutant concentration of each street in the area tends to be the same. The determination coefficient of building density and road density on PM_{10} is concentrated at 0.3 in a city park street. The coefficient of determination of each street's building density and road density in residential land for PM_{10} is 0.35. Due to the construction standards of residential areas in Dalian, some sites are located in high-quality economic centers.

In contrast, others are located in sparsely populated areas, and the difference in traffic flow causes differences in pollutant emissions. The final verification results are the same as the coupling discussed above, which proves the above effect of R^2. Scholars such as Brock believe that increasing population density will worsen the polluted environment [32].

4.4. Discussion

Under the combined influence of industrial emissions and regional traffic, some areas in the main urban area of Dalian are seriously polluted. This result suggests that the compact urban form and monocentric urban layout can attenuate the concentration of pollutants. The distribution of PM_{10} and NO_2 in Dalian conforms to the characteristics of pollution changes in North China. Combined with the attributes of Dalian as a coastal city, a prediction model combined with chemistry can be used for simulation. Since meteorological conditions can control the concentration of pollutants [33], reducing the damage of pollutants to the human body by controlling the population weight of the main urban area of Dalian is feasible [34]. As a two-peak planning functional area with a compact layout, the main urban area has a large difference in topography and building density distribution, so the distribution of pollutants is also very different.

Combined with the measured points in the main urban area, the PM_{10} concentration is higher in some areas where the heat island effect is not apparent [35]. At the same time, areas with higher mobility have higher concentrations of pollutants [36]. In the tourist area of Dalian, the passenger flow in the coastline area is large. Still, the pollutant concentration is low because of the control of pollutant concentration by the sea breeze circulation [37]. This also explains that the air quality inside the Dalian city block is not as good as in the coastal area.

In addition, investment in top industry services can effectively reduce pollutant emissions [38]. At the same time, combined with the low-concentration phenomenon near the coastline of Dalian, high-emission industries are concentrated in the areas eliminated by sea wind energy, which can effectively prevent the concentration of air pollutants from exceeding the standard. Collecting satellite remote sensing data can detect areas with high concentrations of pollutants in cities. Adding green service facilities in the blocks of Dalian can also change the flow of contaminants in the blocks [39].

The concentration of pollutants can also reflect a certain degree of economic development, because contaminants are generated in the production process of enterprises. Urban lockdowns for COVID-19 have significantly reduced nitrogen dioxide emissions from major polluting companies in China [40]. However, although the NO_2 emission concentration in Korea dropped sharply [41], and the AQI decreased significantly, the Health Index increased [42]. In England, rising pollution concentrations can significantly increase infectivity and mortality from COVID-19 [43].

This also reflects the short-term optimization of air pollution in Chinese cities due to the control of COVID-19 [44]. With the short-term closure of Dalian during the epidemic period, the traffic flow of people was significantly reduced. Taking the results of the main urban area of Dalian as an example, within 100 m, the road density has an excellent interference effect on the formation of pollutants, and the building density interferes with the concentration of contaminants and wind conditions through flow. In coastal cities such as Dalian, urban planning and construction must implement the regionally balanced development strategy to avoid congested urban centers, prevent large amounts of pollutants, and reduce pollution sources.

5. Conclusions

In previous studies of urban pollutants, separate pollutant components have not been abstracted separately. This study used accurate measurements and simulations to explore urban pollutants' overall spatial distribution map.

The national control station statistics show that the NO_2 concentration is the highest in winter. The reason for this is that Dalian needs heating in winter, and the burning of fuel produces pollutant emissions. The NO_2 concentration in 2017 was close to the level in 2018. Still, among the measured concentrations, the measured concentration in spring 2018 was much higher than in 2017, proving the necessity of data normalization. The measured PM_{10} concentration in summer is much higher than in winter. The analysis shows that the daytime measurement time is the primary time for urban residents to carry out production activities. As the emission source of PM_{10}, traffic exhaust emissions and industrial production emissions are concentrated in this period. In winter, the outdoor weather is cold, and urban residents' travel activities and work hours are reduced.

In terms of the temporal and spatial distribution of the two pollutants, the concentration of PM_{10} was significantly higher in summer than in winter, and the concentration of NO_2 increased year by year, and was considerably higher in 2018 than in 2017. PM_{10} is mainly concentrated in the southern and central parts of Dalian, and NO_2 is primarily concentrated in the northern part of Dalian. The concentrations of the two pollutants in hilly areas are much higher than those in plain areas. The concentrations in economically developed regions are much higher than those in remote areas. Areas with high road density and building density have high concentrations of pollutants.

The regression analysis of the two pollutants shows that at 100 m, 300 m and 500 m, the determination coefficients of road density and building density on the concentrations of the two pollutants continue to decrease, reaching a maximum of 0.48. Among the influencing factors of PM_{10} concentration, road density is stronger than building density. NO_2 concentration is only related to road density. At the block scale, the ranking of the coupling strength of pollutant concentration with road density and building density, from low to high, is parkland, educational land, commercial land, and residential land.

The innovation of this study lies in revealing the changes in individual pollutant concentrations and exploring the coupling relationship between urban morphological parameters and pollutant concentrations. We should seek ways to reduce the concentration of pollutants from urban morphology, in order to optimize the living environment. Accurate measurements will be combined with real-time outdoor spatial environmental parameters in subsequent studies in the future.

Author Contributions: Y.S.: Conceptualization, Validation, Writing—Original Draft, Writing—Review and Editing, Supervision, Funding acquisition. X.W.: Data curation, Writing—Original Draft, Methodology, Formal analysis, Investigation. Q.Z.: Validation, Writing—Review and Editing, Investigation. D.Z.: Data curation, Methodology, Resources, Funding acquisition. X.M.: Project administration, Resources, Funding acquisition. All authors have read and agreed to the published version of the manuscript.

Funding: This work was supported by the Ministry of Science and Technology of the People's Republic of China [grant number 2013FY112500] and the China Scholarship Council [grant number 201906065035].

Institutional Review Board Statement: Not applicable.

Informed Consent Statement: Not applicable.

Data Availability Statement: Not applicable.

Acknowledgments: We express our deepest gratitude to the funding agencies.

Conflicts of Interest: No known competing financial interests or personal relationships could influence the work reported in this manuscript.

References

1. Yin, L. Study on Air Pollution Control in China from the Perspective of Public Health. In Proceedings of the 3rd International Conference On Economics, Social Science, Arts, Education And Management Engineering (Essaeme 2017), Huhhot, China, 29–30 July 2017; Volume 119, pp. 2219–2222.
2. Wu, N.; Wang, Y.; Wu, J.; He, K.; Peng, Y.; Fu, Z. Globalization of China's Air Environmental Protection Industry under the Belt and Road Initiative. *Eng. Sci.* **2019**, *21*, 39–46. [CrossRef]
3. Li, C.; Liu, B. Air pollution embodied in China's trade with the BR countries: Transfer pattern and environmental implication. *J. Clean. Prod.* **2020**, *247*, 119126. [CrossRef]
4. Zheng, S.; Zhou, X.Y.; Singh, R.P.; Wu, Y.Z.; Ye, Y.M.; Wu, C.F. The Spatiotemporal Distribution of Air Pollutants and Their Relationship with Land-Use Patterns in Hangzhou City, China. *Atmosphere* **2017**, *8*, 110. [CrossRef]
5. Zhao, S.P.; Yu, Y.; Yin, D.Y.; Qin, D.H.; He, J.J.; Dong, L.X. Spatial patterns and temporal variations of six criteria air pollutants during 2015 to 2017 in the city clusters of Sichuan Basin, China. *Sci. Total Environ.* **2018**, *624*, 540–557. [CrossRef]

6. Zhang, X.P.; Gong, Z.Z. Spatiotemporal characteristics of urban air quality in China and geographic detection of their determinants. *J. Geogr. Sci.* **2018**, *28*, 563–578. [CrossRef]
7. Wang, S.Y.; Liu, B.B.; Xu, W.X.; Liu, J.J. Research on the Value Evaluation of Modern Historical Buildings: Taking Zhongshan District of Dalian City as an example. *Urban Archit.* **2020**, *17*, 170–174.
8. Hua, H.D. *Research on Ambient Air Quality in Dalian Based on Bayesian Network*; Dalian Maritime University: Dalian, China, 2018; pp. 18–23. (In Chinese)
9. Zikirya, B.; Wang, J.; Zhou, C. The Relationship between CO2 Emissions, Air Pollution, and Tourism Flows in China: A Panel Data Analysis of Chinese Provinces. *Sustainability* **2021**, *13*, 11408. [CrossRef]
10. Goshua, A.; Akdis, C.; Nadeau, K.C. World Health Organization global air quality guideline recommendations: Executive summary. *Allergy* **2022**. [CrossRef]
11. Zhao, B.; Su, Y.; He, S.; Zhong, M.; Cui, G. Evolution and comparative assessment of ambient air quality standards in China. *J. Integr. Environ. Sci.* **2016**, *13*, 85–102. [CrossRef]
12. Zhang, H.Y.; Cheng, S.Y.; Yao, S.; Wang, X.Q.; Wang, C.D. Insights into the temporal and spatial characteristics of PM2.5 transport flux across the district, city and region in the North China Plain. *Atmos. Environ.* **2019**, *218*, 15. [CrossRef]
13. Fan, H.; Zhao, C.; Yang, Y.; Yang, X. Spatio-Temporal Variations of the PM2.5/PM10 Ratios and Its Application to Air Pollution Type Classification in China. *Front. Environ. Sci.* **2021**, *9*, 692440. [CrossRef]
14. Zha, H.; Wang, R.; Feng, X.; An, C.; Qian, J. Spatial characteristics of the PM2.5/PM10 ratio and its indicative significance regarding air pollution in Hebei Province, China. *Environ. Monit. Assess.* **2021**, *193*, 486. [CrossRef] [PubMed]
15. Tui, Y.; Qiu, J.; Wang, J.; Fang, C. Analysis of Spatio-Temporal Variation Characteristics of Main Air Pollutants in Shijiazhuang City. *Sustainability* **2021**, *13*, 941. [CrossRef]
16. Liu, H.; Zhang, X. AQI time series prediction based on a hybrid data decomposition and echo state networks. *Environ. Sci. Pollut. Res.* **2021**, *28*, 51160–51182. [CrossRef] [PubMed]
17. Zhao, C.; Sun, Y.; Zhong, Y.; Xu, S.; Liang, Y.; Liu, S.; He, X.; Zhu, J.; Shibamoto, T.; He, M. Spatio-temporal analysis of urban air pollutants throughout China during 2014–2019. *Air Qual. Atmos. Health* **2021**, *14*, 1619–1632. [CrossRef] [PubMed]
18. Abirami, S.; Chitra, P. Regional air quality forecasting using spatiotemporal deep learning. *J. Clean. Prod.* **2021**, *283*, 125341. [CrossRef]
19. Gadzhev, G.; Ganev, K. Computer Simulations of Air Quality and Bio-Climatic Indices for the City of Sofia. *Atmosphere* **2021**, *12*, 1078. [CrossRef]
20. Abulude, F.O.; Damodharan, U.; Acha, S.; Adamu, A.; Arifalo, K.M. Preliminary Assessment of Air Pollution Quality Levels of Lagos, Nigeria. *Aerosol Sci. Eng.* **2021**, *5*, 275–284. [CrossRef]
21. Tella, A.; Balogun, A.; Faye, I. Spatio-temporal modeling of the influence of climatic variables and seasonal variation on PM10 in Malaysia using multivariate regression (MVR) and GIS. *Geomat. Nat. Hazards Risk* **2021**, *12*, 443–468. [CrossRef]
22. Wang, C.; Wang, Z.; Zhang, X. Speciated atmospheric mercury during haze and non-haze periods in winter at an urban site in Beijing, China: Pollution characteristics, sources, and causes analyses. *Atmos. Res.* **2021**, *247*, 105209. [CrossRef]
23. Yang, J.Y.; Shi, B.X.; Zheng, Y.; Shi, Y.; Xia, G.Y. Urban form and air pollution disperse: Key indexes and mitigation strategies. *Sustain. Cities Soc.* **2020**, *57*, 10. [CrossRef]
24. Tong, L.; Ji, L.; Li, D.; Xu, H.H. The occurrence of COVID-19 is associated with air quality and relative humidity. *J. Med. Virol.* **2021**, *94*, 965–970. [CrossRef] [PubMed]
25. Wang, Y.Z.; Bechle, M.J.; Kim, S.Y.; Adams, P.J.; Pandis, S.N.; Pope, C.A.; Robinson, A.L.; Sheppard, L.; Szpiro, A.A.; Marshall, J.D. Spatial decomposition analysis of NO_2 and PM2.5 air pollution in the United States. *Atmos. Environ.* **2020**, *241*, 8. [CrossRef]
26. Bechle, M.J.; Millet, D.B.; Marshall, J.D. Does Urban Form Affect Urban NO_2? Satellite-Based Evidence for More than 1200 Cities. *Environ. Sci. Technol.* **2017**, *51*, 12707–12716. [CrossRef] [PubMed]
27. Yan, C.; Wang, L.; Zhang, Q. Study on Coupled Relationship between Urban Air Quality and Land Use in Lanzhou, China. *Sustainability* **2021**, *13*, 7724.
28. Wang, F.; Peng, Y.; Jiang, C. Influence of Road Patterns on $PM_{2.5}$ Concentrations and the Available Solutions: The Case of Beijing City, China. *Sustainability* **2017**, *9*, 17. [CrossRef]
29. Zhao, X.; Shang, Y.P.; Song, M. What kind of cities are more conducive to haze reduction: Agglomeration or expansion? *Habitat Int.* **2019**, *91*, 13. [CrossRef]
30. Yuan, M.; Song, Y.; Huang, Y.P.; Hong, S.J.; Huang, L.J. Exploring the Association between Urban Form and Air Quality in China. *J. Plan. Educ. Res.* **2018**, *38*, 413–426. [CrossRef]
31. Zeng, J.; Liu, T.; Feiock, R.; Li, F. The impacts of China's provincial energy policies on major air pollutants: A spatial econometric analysis. *Energy Policy* **2019**, *132*, 392–403. [CrossRef]
32. Borck, R.; Schrauth, P. Population density and urban air quality. *Reg. Sci. Urban Econ.* **2021**, *86*, 103596. [CrossRef]
33. Zhan, J.Q.; Chang, W.Y.; Li, W.; Wang, Y.M.; Chen, L.Q.; Yan, J.P. Impacts of Meteorological Conditions, Aerosol Radiative Feedbacks, and Emission Reduction Scenarios on the Coastal Haze Episodes in Southeastern China in December 2013. *J. Appl. Meteorol. Climatol.* **2017**, *56*, 1209–1229. [CrossRef]
34. Yuan, M.; Song, Y.; Hong, S.J.; Huang, Y.P. Evaluating the effects of compact growth on air quality in already-high-density cities with an integrated land use-transport-emission model: A case study of Xiamen, China. *Habitat Int.* **2017**, *69*, 37–47. [CrossRef]

35. Yuan, M.; Huang, Y.P.; Shen, H.F.; Li, T.W. Effects of urban form on haze pollution in China: Spatial regression analysis based on $PM_{2.5}$ remote sensing data. *Appl. Geogr.* **2018**, *98*, 215–223. [CrossRef]
36. Wei, L.; Schmitz, S.; Becker, S.; Niehoff, N.; Schwartzbach, F.; von Schneidemesser, E. Climate change and air pollution: The connection between traffic intervention policies and public acceptance in a local context. *Environ. Res. Lett.* **2019**, *14*, 11. [CrossRef]
37. Wei, X.L.; Liu, Y.W.; Liu, Y.B.; Li, L. Numerical study of a local $PM_{2.5}$ pollution event under the typhoon Neoguri (1408) background over a coastal metropolitan city, Shenzhen, China. *Phys. Chem. Earth* **2019**, *110*, 99–108. [CrossRef]
38. Shi, K.F.; Wang, H.; Yang, Q.Y.; Wang, L.; Sun, X.F.; Li, Y.Q. Exploring the relationships between urban forms and fine particulate ($PM_{2.5}$) concentration in China: A multi-perspective study. *J. Clean Prod.* **2019**, *231*, 990–1004. [CrossRef]
39. Tan, H.H. The importance of green infrastructure for improving the air quality of Ho Chi Minh city. *IOP Conf. Ser. Earth Environ. Sci.* **2021**, *779*, 012085. [CrossRef]
40. He, C.; Yang, L.; Cai, B.; Ruan, Q.; Hong, S.; Wang, Z. Impacts of the COVID-19 event on the NOx emissions of key polluting enterprises in China. *Appl. Energy* **2021**, *281*, 116042. [CrossRef] [PubMed]
41. Koo, J.-H.; Kim, J.; Lee, Y.G.; Park, S.S.; Lee, S.; Chong, H.; Cho, Y.; Kim, J.; Choi, K.; Lee, T. The implication of the air quality pattern in South Korea after the COVID-19 outbreak. *Sci. Rep.* **2020**, *10*, 224621. [CrossRef]
42. Seo, J.H.; Kim, J.S.; Yang, J.; Yun, H.; Roh, M.; Kim, J.W.; Yu, S.; Jeong, N.-N.; Jeon, H.W.; Choi, J.S.; et al. Changes in Air Quality during the COVID-19 Pandemic and Associated Health Benefits in Korea. *Appl. Sci.* **2020**, *10*, 8720. [CrossRef]
43. Travaglio, M.; Yu, Y.; Popovic, R.; Selley, L.; Leal, N.S.; Martins, L.M. Links between air pollution and COVID-19 in England. *Environ. Pollut.* **2021**, *268*, 115859A. [CrossRef]
44. He, G.; Pan, Y.; Tanaka, T. The short-term impacts of COVID-19 lockdown on urban air pollution in China. *Nat. Sustain.* **2020**, *3*, 12. [CrossRef]